Nanotechnology Perceptions
ISSN 1660-6795
www.nano-*ntp.com*

Corrosion Studies On Friction Welding Of Dissimilar Metals Cu And Al With Nickel Inter Layer

E. Ravikumar[1, a*], S. Thamizhmani [2, b], R. Palani [3, c], S. Ramalingam [4, d] S.Sarbuddinali [5, e]

[1, 2, 4, 5] *Department of Mechanical Engineering (Deemed to be University), AMET University, Chennai-112, India.*
[3] *Department of Mechanical Engineering, Vel Tech High Tech Dr.Rangarajan Dr.Sakunthala Engineering College (of Anna University), Chennai - 62, India*
[a*]*ravikumar@ametuniv.ac.in,*[b]*siva@ametuniv.ac.in,*[c]*palani@velhightech.com,*[d]*sengalaniramali ngam@amet univ.ac.in*

Friction welding successfully joined Cu-Ni-Al 6061 rods, demonstrating strong mechanical integrity with no separation observed at the joint interfaces after corrosion testing. The study adhered to ASTM G3 standards and examined the pitting corrosion behaviour of AA 6061 in a 3.5 wt% NaCl solution using electrochemical methods such as potentiodynamic polarization. This investigation highlights the complex interplay between upset pressure, microstructure, and corrosion behaviour in friction-welded Cu-Ni- Al 6061 joints. Lower upset pressures tend to enhance corrosion resistance by reducing grain refinement and minimizing plastic deformation, whereas higher pressures, although mechanically beneficial, may increase corrosion susceptibility. SEM analysis did not reveal any large cracks, voids, or separations at the weld interfaces, confirming the mechanical integrity of the joints in a corrosive environment.

Keywords: Friction pressure, Burn off length, Interlayer, potentiodynamic, SEM Analysis.

Introduction

Understanding the evolution of the microstructure from the as-cast dendritic form to the wrought state is essential for optimizing the mechanical properties of nickel-copper alloys. The initial compositional gradients and their subsequent influence on microstructural features play a pivotal role in determining how these materials perform in various applications, particularly in corrosive and high-stress environments. The interplay between solidification processes, mechanical treatments, and microstructural characteristics is foundational in the design and use of these alloys.The 6xxx series aluminum alloys are extensively utilized in the aerospace industry due to their llightweight nature and advantageous structural characteristic.[1] Nevertheless, these metals are prone to localized degradation and fracture due to stress in harsh environments, like saltwater spray and saline mist [2].Friction welding offers a solution to reduce for creation o f fragile intermetallic

compounds at the interface, as it operates under high pressure, has a short processing time, and maintains processing temperatures below the melting point.[3] For instance, Garcia and colleagues examined the resistance to localized corrosion resistance of different regions in welded joints of austenitic stainless steels (AISI 304/316L) in an acidic chloride-containing solution using potentiodynamic anodic polarization and cyclic potentiodynamic polarization techniques. Their findings indicated that the pitting corrosion of the weld metals was greater than that of the base metal [4]. Bimes et al. investigated the pitting corrosion behavior of martensitic welds in chloride environments through potentiodynamic methods and identified the heat-affected zone (HAZ) being the most crucial for localized corrosion, whereas the primary metal remained in a more stable condition

[5] 6061 aluminium alloys, characterized by significant additions of zinc along with magnesium or a combination of magnesium with copper and nickel, exhibit varying levels of strength. Among these, those containing copper and nickel demonstrate thehighest strength, making them suitable for applications in construction, food industries, and aerospace for over 50 years[6]As heat-treatable alloys, the 6xxx series provides moderate strength while offering high resistance to general corrosion, comparable to that of non-heat-treatable alloys[7] When aluminum bonds with copper, intermetallics compounds may form, potentially diminishing corrosion resistance. To enhance the corrosion resistance at the interface between aluminum and copper, the addition of an interlayer is necessary

2. Experimental Work

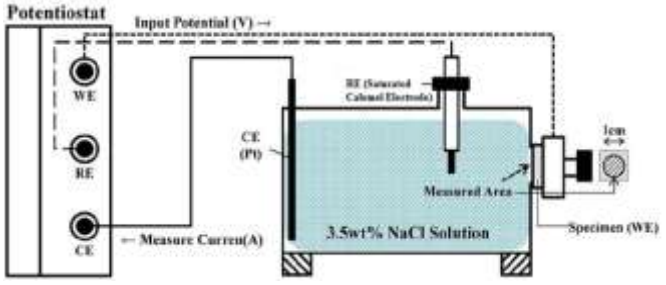

Fig.1: Experimental setup

In this study, friction welding was employed to join dissimilar metals processed aluminum alloy 6061, refined copper, and nickel having a diameter of 19 mm. The chemical composition and mechanical properties of the base metals and nickel interlayer were provided in Tables 1, 2, and 3. The welding process was designed using the Taguchi L9 orthogonal array, which optimizes the parameters across three levels and four key factors to achieve effective joints. Among the nine combinations of parameters tested, four samples were selected for further corrosion, microstructural, and macrostructural analysis, as well as scanning electron microscopy (SEM) examinations. Based on the details you provided, the SEM instrument is likely a ZEISS scanning electron microscope, commonly used in research institutions like the Crystal Growth Centre. The Taguchi method for

designing experiments is widely utilized to enhance the quality of material manufacturing by optimizing process parameters, thereby reducing both experimentation time and cost. The orthogonal array approach ensures optimal parameter settings that remain robust against variations in environmental conditions and other noise factors. The selected samples were mechanically polished and etched with a 3.5% nital solution (for aluminum and nickel) and an aqueous solution of 100 g/L sodium met bisulfite (for copper) to reveal their microstructures. Inverted metallurgical optical microscopy with magnifications ranging from 100x to 600x was used for microstructural analysis, allowing for detailed observation of grain structure, phase boundaries, and interface zones. Polishing was conducted using sandpaper and diamond pastes to ensure a smooth surface, followed by ultrasonic cleaning in acetone to remove contaminants.

2.1 Corrosion Testing

Specimens of 75 mm length and 19 mm diameter were used, with surfaces polished utilizing 1μm diamond particles. After polishing, the specimens were ultrasonically cleaned and weighed utilizing a high precision scale as precise as0.0001. Immersion tests were conducted in a neutral 4% NaCl solution for 24 hours, after which the corrosion products were removed using a soft brush. Weight loss was measured to determine the corrosion rate. The specimens were rinsed, dried, and weighed again post-immersion to calculate the weight loss, which was employed to assess the corrosion rate of every sample. Conducted under standard ASTM procedures, the polarization tests were carried out to evaluate the electrochemical behavior of the friction- welded joints and compare them to the parent metals. A saturated calomel electrode (SCE) was used as the reference electrode in the electrochemical cell setup. The potentiodynamic tests assessed the corrosion potential (Ecorr), corrosion current density (Icorr), and polarization resistance, providing detailed insights into the corrosion mechanism at the weld interface and heat-affected zones (HAZ).

2.2 Electrode Preparation

The working electrode was prepared from friction-welded samples measuring 1 cm x 1 cm, cut from cylindrical specimens using a Wire EDM process. Samples were polished with different grades of emery paper to remove surface impurities and achieve a smooth, conductive surface for electrochemical testing. The corrosive environment used was a neutral 3.5% sodium chloride (NaCl) solution, simulating saline conditions that typically accelerate corrosion. The polarization curves were obtained by varying the potential from –250 mV to +250 mV relative to the open-circuit potential (Ecorr) at a scan rate of 0.5 mV/s. Experiments were performed at ambient temperature (25°C), using a 60-minute delay before the polarization scan to allow the system to reach an equilibrium condition. Meanwhile, both voltage vs. time and current vs. time were measured to ensure system's stability. The weld metal exhibited superior corrosion resistance compared to the TMAZ and the base metal. This was evident from parameters such as the corrosion potential (Ecorr) and corrosion current density (Icorr). The corrosion potential (Ecorr) for the weld metal was more positive, indicating better resistance to corrosion initiation. In contrast, the TMAZ and base metal exhibited lower (more negative) Ecorr values, signifying higher

susceptibility to corrosion. The corrosion current density (Icorr), which reflects the rate of material dissolution in the corrosive environment, was lower for the weld metal compared to the TMAZ and base metal. This suggests that the friction-welded zone has better electrochemical stability and a more protective passive layer, resulting in slower corrosion kinetics.

2.3 Microstructure observation

Figure displays the microstructure of samples annealed for various durations, illustrating a microstructure consisting predominantly of aluminum (Al). The optical micrographs reveal the growth of recrystallized aluminum grains as a function of annealing time. Quantitative analysis was conducted to measure the grain diameter of samples recrystallized at different times, highlighting the correlation between annealing duration and grain size. 2(a), 2(b) and 2 (c)

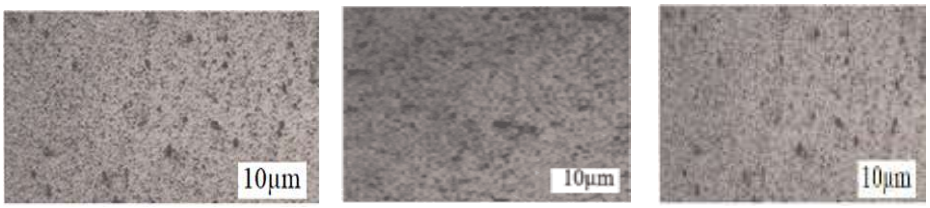

Fig. 2. Microscopic Analysis AA6061 aluminum After recrystallization heat treatment at 250°C for (a) 4 minutes, (b) 13 minutes, (c) 20 minutes

2.4 Grain Size and Metastable Pitting Frequency

Experiments involving potentiostatic polarization of 6061 aluminum samples with varying grain sizes show that grain refinement can significantly influence the frequency of metastable pitting. Grain refinement leads to a higher density of grain boundaries, which promotes the formation of a stable passive film. A finer grain structure offers more surface area for passive film formation, resulting in greater electrochemical stability. For instance, in Fe alloys, a chromium-rich passive film is more stable in finer-grained microstructures due to enhanced Cr diffusion into the passive layer [21-24]

Design of Experiments (DOE)

Table 1 Chemical Composition of Aluminum Alloy AA6061-T6

ELEMENTS	Cu	Pb	Sn	Fe	Ni	Te
WT %	99.73	0.003	0.184	0.080	0.068	0.018

Table 2Chemical Composition of pure Copper

ELEMENTS	SI	FE	CU	Mn	Cr	AL
WT %	0.4 - 0.8	0.0 - 0.7	0.15 - 0.4	0.0 - 0.15	0.04 - 0.35	95.85 - 98.56

Table 3 Chemical Composition of Pure Nickel

ELEMEN TS	Al	Mn	Si	Mo	Cr	Ni
WT %	0.033	0.003	0.002	0.004	0.002	99.5

Table4. Corrosion Test Input Parameters

Sl. No.	**Upset Pressure (in tons)**	**Friction Pressure**	**Burn-off length (in mm)**	**Speed of Spindle (in rpm)**	**Remarks**
1	2.5	1.3	1	2000	Cu doesn't weld properly
2	2.6	1.5	2	1000	Cu doesn't weld properly
3	2.7	1.7	3	1500	Cu came out on machining
4	**2.8**	**1.8**	**2**	**1500**	
5	**2.9**	**1.9**	**3**	**2000**	
6	**3.0**	**1.9**	**1**	**1000**	
7	**2.0**	**2.0**	**3**	**1000**	
8	3.1	2.1	2	1500	Cu came out on machining
9	3.2	2.2	2	2000	Cu did not weld

Welding sample Images

Fig 3. Aluminium + Nickel welding

Fig 4. Aluminium+ Copper welding

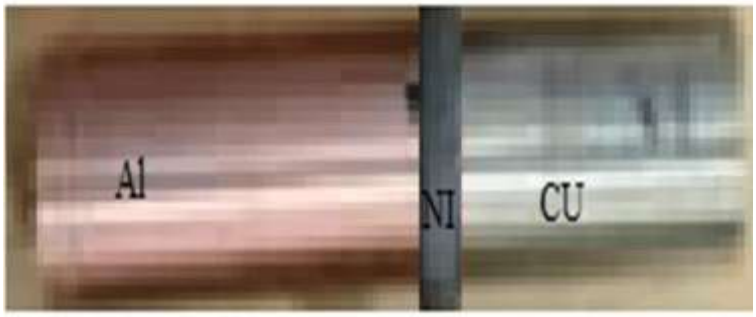

Fig 5. After welding AL+ NI+ Cu

Table5. These parameters are considered to investigate corrosion test

S No	Sample no	Friction Pressure (MPa)	Upset pressure (MPa)	Burn-off length (mm)	Speed (RPM)
1	4	2.8	1.8	2	1500
2	5	2.9	1.9	3	2000
3	6	3.0	1.9	1	1000
4	7	2.0	2.0	3	1000

Table6 -corrosion output parameters

Sample No;	I corr m/Sq cm	Rest potential	Reverse potential	Corrosion rate	Remarks

Sample No: 4 Upset pressure-2.8, Friction Pressure-1.8, Burn of length-2, R.P.M-1500	37.408	-722.46	250 mV	870.12(mm/year 34256(mil/year	Cu-Ni-Al
Sample No: 5 UP-2.9, FP-1.9, BOL- 3, RPM-2000	36.69	-721.96	250 mV	412.03(mm/year 16221(mil/year	Cu-Ni-Al
Sample No: 6 UP-3. FP1.9,BOL- 1, RPM-1000	356.64	-728.03	250mV	8295.5(mm/year 326590(mil/year	Cu-Ni-Al Copper not welded
Sample No: 7 UP-2.0,FP- 2.0,BOL- 3 RPM-1000	0.4659457	-733.97	250mV	5.2325(mm/year 206.0(mil/year	Cu-Ni-Al
Sample No: Cu Base	209..37	-291.99	250mV	4870.1(mm/year) 191730 (mil/year)	Cu
Sample No: Al Base	558.82	-734.65	250mV	6275.5(mm/year) 247070(mil/year	Al

Result and Discussion

The friction welding parameters used for sample No: 7, which consists of Cu-Ni-Al, yielded the least corrosion rate among the tested samples. The corrosion current (ICorr) for this sample was measured at 0.466 mA/cm², indicating a lower rate of corrosion. This result suggests that the selected parameters for friction welding effectively enhanced the corrosion resistance of the Cu-Ni-Al sample.

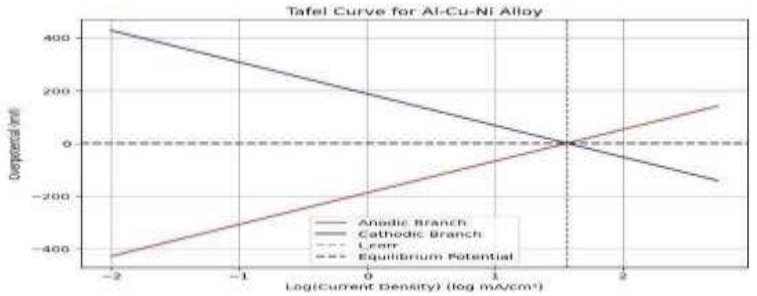

Fig.6 Electrochemical Polarization graph for Al-Ni-Cu (Sample No: 7)

The Tafel polarization curve is a widely used electrochemical technique for evaluating the corrosion behaviour of materials. This particular graph represents the Al-Cu-Ni alloy, depicting its anodic and cathodic reactions in an electrolyte. X-Axis (Current Density) (log mA/cm²) represents the logarithmic scale of current density, indicating the rate of the electrochemical reaction. A higher current density corresponds to a more aggressive corrosion reaction. Y-Axis Over potential (mV), the deviation of the electrode potential

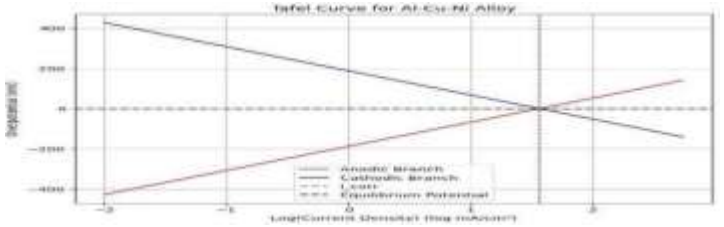

from its equilibrium value due to polarization. Positive values indicate anodic polarization (metal dissolution), while negative values indicate cathodic polarization (reduction reactions). Anodic red curve represents the metal oxidation reaction, where the Al-Cu-Ni alloy dissolves into ions. As the potential increases, the anodic current density rises, signifying higher metal dissolution and corrosion rate. Cathodic Blue curve represents the reduction reaction, as the potential decreases, the cathodic current density increases, indicating a more active reduction process. The intersection of the anodic and cathodic curve represents the equilibrium potential where the rate of oxidation (metal dissolution) equals the rate of reduction. Sample No.6 exhibits the maximum corrosion rate at the interface. The corresponding corrosion current, referred to as I_Corr, is notably high at 356.64Ma/cm2

Fig.7 Polarization Curve for Al-Ni-Cu (Sample No: 6)

A shorter burn-off length (BOL- 1mm) sample 6, typically results in less material being fused at the interface. This could lead to weaker bonds, reduced fusion depth, and possibly more exposure of the base materials to the corrosive environment. However, the use of lower rotational speed likely compensated for this by providing a better overall weld quality. Lower speed reduces thermal gradients and minimizes defects, which may counteract some of the issues caused by a shorter burn-off length. Corrosion Performance of Samples 4 & 5 reveals that the intermediate corrosion rates and currents (37.408 mA/cm² and 36.69 mA/cm² with corresponding corrosion rates of 870.12 mm/year) indicate that these samples were neither the best nor the worst performers. This suggests that their welding parameters, while adequate, may not have been optimized to achieve the highest corrosion resistance.

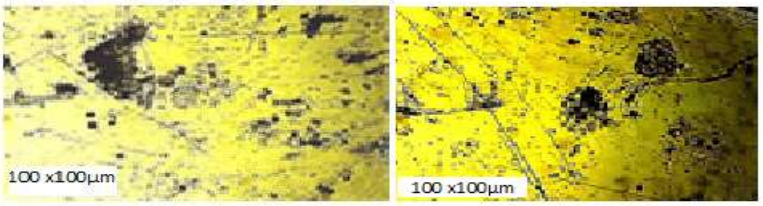

Fig.8. Microstructure Al-Ni-Cu (sample No.7) (after decomposition Nickel-Aluminum Alloy Interface (Fig. 7b,)

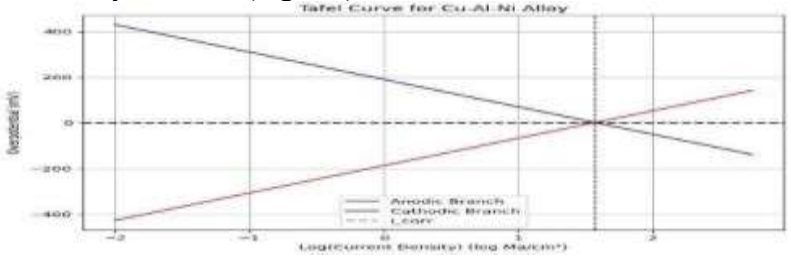

Fig. 9. Polarization curve Al-Ni-Cu

Fig. 9, showing the Tafel curve illustrates the electrochemical polarization behavior of a Cu-Al-Ni alloy, a material commonly used in marine, aerospace, and structural applications due to its corrosion resistance. This curve is essential for evaluating the corrosion rate and electrochemical kinetics of the alloy in a given electrolyte. The x-axis represents the logarithm of current density (log mA/cm²), which signifies the rate of charge transfer occurring due to oxidation and reduction reactions. A higher current density indicates a more significant reaction rate, directly influencing corrosion susceptibility. The y-axis denotes the electrode potential (mV vs. a reference electrode), which reflects the energy level of the metal surface and its tendency to gain or lose electrons. Using nickel as an interlayer between aluminum and copper improves the corrosion resistance of the joint. Nickel serves as a barrier that prevents direct contact between aluminum and copper, which helps in reducing galvanic corrosion. Nickel's corrosion-resistant properties also protect the joint from aggressive environments, such as chloride-containing solutions. When aluminum and copper are directly joined, they form a galvanic couple, where aluminum, being more anodic, corrodes faster in the presence of an electrolyte (such as water or salt). Adding nickel helps mitigate this effect by acting as an intermediary that reduces the galvanic potential difference between aluminum and copper The metallurgical connectivity of aluminum, nickel, and copper in friction welding or other joining processes is influenced by their differences in melting points, thermal conductivity, and oxidation behaviour. Friction welding is a suitable method for joining these dissimilar metals, as it mitigates the formation of brittle intermetallic compounds and provides a strong bond with improved corrosion resistance when nickel is used as an interlayer. Proper control of welding parameters is critical to optimize the joint quality, mechanical strength, and resistance to corrosion

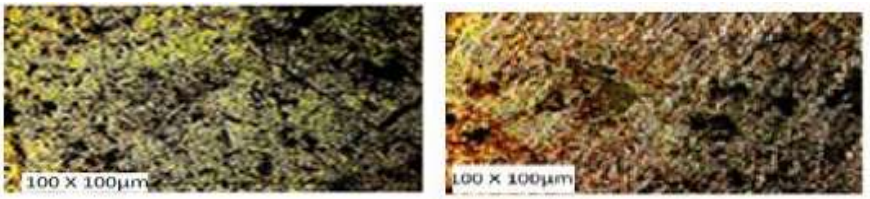

Fig. 10 Microstructure Al-Ni-Cu (sample No.4) (after corrosion)

Fig.10 Depicting the microstructure of the Al-Ni-Cu alloy (Sample No: 4) after corrosion testing, likely shows significant differences compared to Sample No. 7. For Sample No: 4, might observe Extensive Corrosion Deep pits and extensive surface degradation indicating poor corrosion resistance. Prominent oxidation patterns and possibly a roughened surface. Alterations in phase distribution or morphology due to corrosion, nickel's excellent corrosion resistance and the effectiveness of the parameters used for Sample No. 7 are clearly demonstrated. Nickel's resistance to corrosion is a significant factor in the performance of the friction- welded joints. The optimal parameters for Sample No. 7, 2 bar upset pressure, 2 bar friction pressure, 3 mm burn-off length, and 1000 RPM (Refer table6) appear to be effective in enhancing corrosion resistance by leveraging the properties of nickel. Comparing the microstructures confirms that the nickel interface and the parameters used for Sample No. 7 results in minimal corrosion damage, supporting their selection as ideal for reducing corrosion in friction welding processes.

Fig.11 Base metal Aluminum alloy.

Showing the base metal aluminum alloy's polarization curve is important for analyzing its corrosion behavior. From this graph, we can infer the corrosion resistance of the Aluminum alloy in a given environment. If the corrosion current I_corr is high, it indicates a higher corrosion rate, suggesting that the alloy is more susceptible to degradation. Conversely, a lower I_corr implies better corrosion resistance. This information is crucial for selecting materials in marine, aerospace, and industrial applications where aluminum alloys are commonly used

Fig. 12 Microstructure Al (After corrosion)

Shows, depicting the microstructure of aluminum (Al) after corrosion, provides valuable insights into how aluminum performs under corrosive conditions. Corrosion Damage**,** Examine the extent of surface damage, including pits, cracks, and general erosion. Significant corrosion damage would indicate poor resistance. Look for signs of oxidation, such as a roughened or discolored surface. Aluminum typically forms an oxide layer, but extensive corrosion might compromise this layer. Assess if there are any changes in the microstructure, such as phase transformations or dissolution of certain phases, which can affect corrosion resistance. Identify any corrosion products that have formed on the surface. David Talbot and James Talbot
[9] Highlighted the formation of Protective oxide layer films on aluminum alloys and the impact Of chloride ions on corrosive behavior. Kenneth R. et al, Demonstrated that chloride ions significantly increase corrosion rates, emphasizing the importance of controlling the corrosive environment. Venugopal et al.: Found that friction stir welds of AA7075 alloy exhibit better corrosion resistance than TMAZ and base metals in a 3.5% NaCl solution. Srinivasarao and Prasad Rao, Used Tafel curve extrapolation to analyze pitting corrosion in AA6061 and nickel, providing insights into corrosion potential (Ecorr) and corrosion current (Icorr).[10] Polarization resistance measurements are indeed a valuable tool for evaluating corrosion rates and understanding material performance under different corrosive conditions. These studies collectively reinforce the importance of both material selection and corrosion testing in optimizing the performance of aluminum alloys in challenging environments. Venugopal et al. [11] investigated the microstructural characteristics and pitting corrosion behavior of friction stir-welded AA7075 aluminum alloy in a 3.5% NaCl solution. Their findings indicated that the weld metal exhibited superior corrosion resistance compared to the thermomechanically affected zone (TMAZ) and the base metal. Similarly, Srinivasarao and Prasad Rao [12] analyzed the pitting corrosion mechanism using the Tafel curve extrapolation method, which was applied to samples 6 and 7.

Fig.13 Friction welded Al-Ni-Cu (Sample No.7)

Copper exhibits fine grains on macro etching, indicating significant thermal influence. A layer of plastically deformed copper is located at the interface between nickel and aluminum alloy, suggesting considerable mechanical interaction and material flow. Aluminum Alloy demonstrates good grain flow under the process's heat and pressure, indicating effective deformation and recrystallization. Recrystallization is visible, with well-resolved grains Nickel displays fine pitting marks, likely Due to high heat input., which could have impacted the material's surface integrity. Appears to be more resistant to gross deformation compared to aluminum but is still affected by the heat. These observations reveal that a complex interaction between the materials at the interface, with copper being more susceptible to heat effects, while aluminum and nickel show distinct responses in terms of grain structure and recrystallization

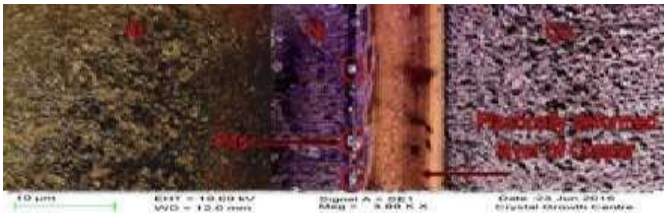

Fig. 14. Friction welded Al-Ni-Cu (Sample No. 6)

This analysis can provide insights into the mechanical properties and corrosion behavior of the welded joint. The image appears to be a macro or micrograph of a friction-welded sample, likely showing the interface between aluminum (Al), nickel (Ni), and copper (Cu). The grain structure in the aluminum region seems relatively uniform, with no visible eutectic grains, supporting your earlier observation of eutectic particle dissolution in the heat-affected zone (HAZ) The nickel region shows the presence of pits, as indicated by the red circles in the image. These pits are likely a result of localized corrosion or excessive heat input during the welding process, leading to surface imperfections. The copper region exhibits a distinct texture with fine grains visible, which aligns with your previous observations of fine grains in the HAZ of copper after macro etching. There is a clearly visible layer of plastically deformed copper at the interface between nickel and aluminum. This layer suggests significant mechanical deformation and flow of the copper material during the friction welding process. The interface between the materials is well-defined, with clear transitions between the aluminum, nickel, and copper regions. The image shows how the materials have interacted under the thermal and mechanical effects of friction welding. Sample **7** shows a significantly lower corrosion rate (5.2325 mm/year) compared to Sample 6 (8295.5 mm/year), indicating better corrosion resistance, likely due to the optimized welding parameters and the presence of the Nickel interlayer.

5. Conclusion

The investigation into the corrosion behavior of the Nickel (Ni) interlayer on aluminum copper provided several key insights

1. The weld, thermomechanically affected zone (TMAZ), and heat-affected zone (HAZ)

exhibit a higher equilibrium potential, indicating greater corrosion resistance compared to the parent metal. This enhanced resistance may result from microstructural modifications induced by the welding process.

2. Potentiodynamic measurements reveal that grain size variation has minimal influence on the pitting potential of AA6061 aluminum in a 3.5 wt% sodium chloride solution. This indicates that factors like alloy composition and surface condition have a greater impact on pitting resistance.

3. SEM analysis revealed that Sample 6 experienced severe corrosion in the fusion zone, with deep pits forming along the interface, whereas Sample 7 showed less severe corrosion.

4. This emphasizes the significance of the Nickel interlayer in reducing corrosion in these critical regions. The Aluminum matrix shows finely distributed pits as a result of the corrosion process, with a higher pit density in samples lacking the Nickel interlayer. This further reinforces the Nickel interlayer's protective role in improving corrosion resistance.

6. References

[1] B. S Yilbas, A. ZSahin , N. Kahraman, and A.Z.Al- Gami: J. Mater. Process. Technol, 49, 1995
[2] G.Mahendran, V.Balasubramanian,T.Senthilvelan, Influences of diffusion bonding process parameters on bond characteristics of Mg-Cu dissimilar joints, Trans.Nonferrous Met.Soc.China,2010,20, pp997-1005
[3] Won-B. Lee, Kuck- saeng Bang,Seung- Boo Jung Journal of Alloys of compounds, 390 (2005)
[4] Garcia C, Martise F, De Tiedra P, Blanco Y, Lopez M, Corros sci2008:50:1184-94
[5] BilmesPD,Llorente CL, Mendez CM, Garvasi CA CorrosSci 2009;51:876-81
[6] J G Kaufman and E.L Rooy, corrosion test and standards, Applications and Interpretation,2nd edition, edited by R. Baboian, ASM International, Material park, OH, (2005) 1-8.
[7] G. Kufman, in ASM Hand book, Volume 13 B, Corrosion: Materials,edited by S.D. Cramer and B.S. Covino Jr. ASM International, Material park,OH (2005) 95 -124.
[8] I. J Park,S.T Kims, I.S. Lee, Y.S. Park, M.B.Moon,Mater. Trans. (JIM) 50 (2009)
[9] David Talbot and james Talbot, Corrosion Science and Technology,CRC Press LIC,1998
[10] R Kenneth, Trethwey and J.Chamberlain,Corrosion for Science and Engineering, Long man Group limited,2nd Edition,1996.
[11] T.Venugopal,K. Srinivasarao,andK.Prasadrao, Trans Inst. Metals, 57(2004) 659-663.
[12] K.Srinivasa Rao and K.Prasad Rao, Transaction of Indian Institute of metals, 57(2004) 503-610.
[13] G.S Frankel, L. Stockert, F,Hunkeler, H.Boehni,Metastable Pitting of Stainless Steel, Corrosion43 (1987) 429-436.
[14] X.Y. Wang, D.Y.Li Mechanical and electrochemical behavior of nanocrystalline surface of 304 Stainless steel, Electrochemical. Acta 47 (2002) 3939- 3947.
[16] W. Zeiger, M. Schneider, D. Scharnweber, H. Worch, Corrosion behavior of a Nanocrystalline FeA18 alloy. Nanostruct. Mater. 6 (1995) 1013-1016.
[17] K.M.S. Youssef, C.C Koch, P.S. Fedkiw, Improved corrosion behavior of nano crystalline zinc produced by pulse- current electodeposition, corros. Sci, 46 (2004) 51-64.
[18] G. Wranglen, pitting and sulphide inclusion in steel, Cerros. Sci 14 (1974) 331-349.
[19] D.E Willaims, J. Stewart, P.H. Balkwill, The nucleation, growth and stability of microptic in stainless steelCorros. Sci 36 (1994) 1213 -1235.
[20] M.H Ras , P.C. Pistorius, possible mechanism for the improvement by vanadium of the pitting corrosion resistance of 18% choromium feritic Stainless steel, Corros.Sci.44 (2002) 2479 -2490.
[21] W Tain, N. Du, S. Li, S. Chen, Q wu, Metastable pitting corrosion of 304 Stainless steel in 3.5% NaCl solution. Corros. Sci 85 (2014) 372-379.

[22] P.C. Pistorius, G.T. Bustein, Aspect of the Effect of electrolyte composition on the occurrence of metastable pitting on stainless steel, Corros. Sci 36 (1994) 525-538.
[30] B. YU, P. Woo, U. Erb, Corrosion behavior of nanocrystalline copper foil in sodium hydroxide solution, Scr. Mater. 56 (2007) 353-356.
[23] Montgomery D (2006) Design and analysis of experiments. John Wiley & Sons, Inc
[24] Ross P (1988) Taguchi techniques for quality engineering. Tata McGraw Hill